DNA-Dependent Protein Kinase Is a Therapeutic Target and an Indicator of Poor Prognosis in B-Cell Chronic Lymphocytic Leukemia

Elaine Willmore,[1] Sarah L. Elliott,[1] Tryfonia Mainou-Fowler,[2] Geoffrey P. Summerfield,[2] Graham H. Jackson,[2] Fran O'Neill,[3] Christopher Lowe,[3] Anthony Carter,[5] Robert Harris,[5] Andrew R. Pettitt,[5] Celine Cano-Soumillac,[1] Roger J. Griffin,[1] Ian G. Cowell,[4] Caroline A. Austin,[4] and Barbara W. Durkacz[1]

Abstract

Purpose: del(17p), del(11q), and associated p53 dysfunction predict for short survival and chemoresistance in B-cell chronic lymphocytic leukemia (CLL). DNA-dependent protein kinase (DNA-PK) is activated by DNA damage and mediates DNA double-strand break repair. We hypothesized that inhibiting DNA-PK would sensitize CLL cells to drug-induced DNA damage and that this approach could increase the therapeutic index of agents used to treat CLL.

Experimental Design: Fifty-four CLL cases were characterized for poor prognosis markers [del(17p), del(11q), CD38, and ZAP-70]. In selected cases, DNA-PK catalytic subunit (DNA-PKcs) expression and activity and p53 function were also measured. *Ex vivo* viability assays established sensitivity to fludarabine and chlorambucil and also tested the ability of a novel DNA-PK inhibitor (NU7441) to sensitize CLL cells to these drugs. The effects of NU7441 on fludarabine-induced DNA damage repair were also assessed (Comet assays and detection of γH2AX).

Results: DNA-PKcs levels correlated with DNA-PK activity and varied 50-fold between cases but were consistently higher in del(17p) ($P = 0.01$) and del(11q) cases. NU7441 sensitized CLL cells to chlorambucil and fludarabine, including cases with del(17p), del(11q), p53 dysfunction, or high levels of DNA-PKcs. NU7441 increased fludarabine-induced double-strand breaks and abrogated drug-induced autophosphorylation of DNA-PKcs at Ser^{2056}. High DNA-PK levels predicted for reduced treatment-free interval.

Conclusions: These data validate the concept of targeting DNA-PKcs in poor risk CLL, and demonstrate a mechanistic rationale for use of a DNA-PK inhibitor. The novel observation that DNA-PKcs is overexpressed in del(17p) and del(11q) cases indicates that DNA-PK may contribute to disease progression in CLL.

A major determinant of poor prognosis and therapeutic resistance in B-cell chronic lymphocytic leukemia (CLL) is dysfunction in the p53-dependent DNA damage response pathway. del(17p), frequently associated with mutation in the remaining p53 allele, is one of the clearest indicators of treatment-refractory CLL, with median treatment-free interval (TFI) of 9 months (1, 2). The mutational status of ataxia telangiectasia mutated kinase (ATM) and associated del(11q) predict reduced overall and treatment-free survival (3). Because ATM is a key upstream regulator of p53, defects in either ATM or p53 (which occur collectively in up to ~30% of patients) lead to an impaired DNA damage response that correlates with therapeutic resistance and reduced survival. Both fludarabine and chlorambucil treatment induce p53 stabilization and p53-dependent apoptosis in CLL cells with wild-type p53 (4–6). Correlations among ATM, p53 status, and therapeutic resistance have been clearly shown; however, their relationships to sensitivity of CLL cells to fludarabine or chlorambucil in *ex vivo* cytotoxicity assays have not been fully addressed.

Chlorambucil-induced cross-links produce DNA double-strand breaks (DSB) during a repair process mediated by nucleotide excision repair and homologous recombination repair (7–9). DNA-dependent protein kinase (DNA-PK) function is specifically required for nonhomologous end joining, the predominant pathway for DSB repair (10). DNA-PK has been implicated in the repair of chlorambucil-induced

Authors' Affiliations: [1]Northern Institute for Cancer Research, [2]Department of Hematology, [3]Institute of Human Genetics, and [4]Institute for Cell and Molecular Biosciences, Newcastle University, Newcastle upon Tyne, United Kingdom and [5]Department of Hematology, University of Liverpool, Liverpool, United Kingdom

Received 12/13/07; revised 2/11/08; accepted 3/4/08.

Grant support: Leukaemia Research, UK grants 07019 and 06055 (E. Willmore and S.L. Elliot).

The costs of publication of this article were defrayed in part by the payment of page charges. This article must therefore be hereby marked *advertisement* in accordance with 18 U.S.C. Section 1734 solely to indicate this fact.

Note: Supplementary data for this article are available at Clinical Cancer Research Online (http://clincancerres.aacrjournals.org/).

Requests for reprints: Elaine Willmore, Northern Institute for Cancer Research, Newcastle University, Newcastle upon Tyne NE2 4HH, United Kingdom. Phone: 44-191-246-4447; Fax: 44-191-246-4301; E-mail: Elaine.Willmore@ncl.ac.uk.

doi:10.1158/1078-0432.CCR-07-5158

cross-links, because increased DNA-PK activity in CLL cells correlates with clinical resistance to chlorambucil (8, 9). Furthermore, nonhomologous end joining and DNA-PK activity are increased in radioresistant compared with radiosensitive CLL cells (11). Combination therapy with fludarabine and cyclophosphamide is effective in CLL because of the inhibitory effect of fludarabine incorporation into repair patches following cyclophosphamide-induced DNA damage (12). Whether specific DNA repair pathways are implicated in the cytotoxic response of CLL cells to fludarabine per se has not been fully investigated.

Several DNA-PK inhibitors have been described (13–16), but they lack the specificity and potency required for clinical use. In collaboration with KuDOS Pharmaceuticals, the Drug Development Group at Newcastle University synthesized and characterized a series of novel DNA-PK inhibitors. Our first inhibitor (NU7026) sensitized cell lines and CLL lymphocytes to ionizing radiation (IR) and topoisomerase II poisons (11, 17, 18). NU7026 also enhanced chlorambucil-induced cytotoxicity in CLL cells (19), and this correlated with increased levels of γH2AX foci, a surrogate marker for DSB. The current benchmark DNA-PK inhibitor, NU7441, shows ATP-competitive inhibition kinetics, has improved potency and selectivity (IC_{50} for *in vitro* DNA-PK inhibition, 13 nmol/L), and increases etoposide-induced tumor growth delay in xenograft models (20, 21). NU7441 showed >100-fold selectivity for DNA-PK over related kinases.[6]

In this study, we hypothesized that targeting DNA-PK (with NU7441) would sensitize CLL cells to drug-induced DNA damage by inhibiting DSB repair. To test this theory, the role of DNA-PK function and expression in CLL was explored using a cohort of 54 cases that were characterized for CD38 and ZAP-70 expression and del(17p) and del(11q) status. Selected samples were further characterized for p53 functionality. *Ex vivo* assays were used to establish the range of drug sensitivities, to assess the efficacy of NU7441 as a chemosensitizer, and to measure drug-induced DNA damage and repair. The data described here validate the concept of targeting DNA-PK in poor prognosis CLL.

Materials and Methods

Patient sample information. Patients had been diagnosed with CLL following standard immunophenotyping and had attended clinics from 2003 to 2006. Informed consent was obtained and the study was carried out under national ethical guidelines. CLL cells were isolated from whole blood using Lymphoprep. Cells were incubated in RPMI 1640 supplemented with 10% (v/v) fetal bovine serum, penicillin (50 units/mL), and streptomycin (50 μg/mL). CD38 and ZAP-70 status were measured (as described previously; refs. 22, 23) in cells that had been frozen (90% fetal bovine serum and 10% DMSO at the time of collection) and samples were classed as positive if the expression was >30% or >20%, respectively. Viability (trypan blue exclusion) was routinely >95% in fresh and thawed samples after 24-h culture. Binet staging refers to the patient status at the time of sample collection. Wherever feasible, prognostic tests and other assays were done with each sample. However, due to small sample size in some cases, this was not always possible.

Cytogenetic analyses. Interphase fluorescence *in situ* hybridization was carried out using commercially supplied probes for p53 (Vysis) and ATM (MP Biochemicals) following the manufacturers' protocols. A minimum of 10% of cells with one target signal and two control signals was used for assigning deletion status to p53 and ATM [in this study, all del(11q) and del(17p) cases contained >25% cells with deletions]. Deletion status was also assessed by a multiple ligation-dependent probe amplification kit (MRC Holland) and analysis using GeneMarker (v 1.51; SoftGenetics). There was 100% concordance between the two techniques (full details to be published separately).

Drugs. Fludarabine and chlorambucil were obtained from Sigma. 4- Hydroperoxycyclophosphamide was a gift from Dr. Susan Ludeman (Duke Comprehensive Cancer Center). NU7441 (8-dibenzothiophen-4-yl-2-morpholin-4-yl-chromen-4-one; ref. 20) and its noninhibitory analogue NU7742 (8-dibenzothiophen-4-yl-2-piperidin-1-yl-chromen-4-one) were obtained from Prof. Roger Griffin and were synthesized as part of a collaboration between the Drug Development Group of the Northern Institute for Cancer Research (Newcastle University) and KuDOS Pharmaceuticals. Full details of the synthesis of NU7442 will be published separately. NU7441 and NU7742 (2 mmol/L) were dissolved in anhydrous DMSO and used in all experiments at final concentrations of 1 μmol/L. This concentration was found to be nontoxic and optimal for inhibition of DNA-PK in previous cell line studies (21).

XTT viability and caspase-3/7 assays. Freshly isolated cells (5×10^5 per well) were seeded into 96-well plates. Drug(s) and solvent controls were added to three to six replicate wells. After 0, 16, or 40 h, caspase-3/7 assays were carried out (Apo-ONE caspase-3/7 kit; Promega; as per manufacturer's instructions). After 5 days, viability was quantified using an XTT kit (Roche) following the manufacturer's protocols. Results were expressed as a percentage of controls. NU7441 alone decreased cell viability in some cases (range, 5-40% after a 5-day incubation). Consequently, replicates treated with inhibitor alone were used as controls in calculations using drug combinations. LC_{50} values (concentration decreasing viability by 50%) were calculated from line graphs. PF_{50} values (potentiation factor at 50% viability) were expressed as a ratio of LC_{50} (drug alone) / LC_{50} (drug + inhibitor).

DNA-PK activity in intact cells (autophosphorylation at Ser^{2056}). Whole-cell extracts were prepared from drug-treated cells (after 24-h exposure). Western blotting was carried out as described below and an antibody to phosphorylated DNA-PK catalytic subunit (DNA-PKcs; Ser^{2056}; Abcam) was used.

DNA-PK* ex vivo *activity assay. This assay measures the ability of DNA-PK to phosphorylate Ser^{15} on p53 and is based on a previously described method (24). Whole-cell extracts (from untreated CLL cells) were prepared and 10 μg protein per reaction were used in a final volume of 40 μL in buffer containing 50 mmol/L KCl, 25 mmol/L HEPES (pH 4), 12.5 mmol/L $MgCl_2$, 10% (v/v) glycerol, 0.05% (v/v) NP-40, and 1 mmol/L DTT together with 1 μg substrate GST-p53N66 (amino-terminal 66 amino acids of p53 fused with glutathione *S*-transferase) and 1 ng/mL 30-mer double-stranded DNA oligonucleotide. Ten microliters of 250 μmol/L ATP were added. After 30 min (30°C), the reaction was stopped with 6 mol/L guanidine. Phosphorylated Ser^{15} was detected using mouse anti-phosphorylated p53 Ser^{15} and horseradish peroxidase–linked secondary antibody (Cell Signaling Technology) in a dot-blot procedure. Detection was by ECL reagent (Amersham) and a Fuji LAS-3000 luminescent image analyzer system. DNA-PK activity was quantified using a standard curve of purified DNA-PK, and activity was represented as nanogram of DNA-PK per microgram of protein extract.

Flow cytometric analysis of p53 function. The principle underlying this assay is described in Results. As described previously (25), CLL lymphocytes were divided into two groups, with half mock-irradiated and half treated with 5 Gy IR. After 14 h, cells were fixed (2% paraformaldehyde) and permeabilized (80% ethanol). A p53 antibody (clone DO-1; Oncogene Research), p21 antibody (clone EA10; Oncogene Research), or isotypic control antibody (Becton Dickinson) was used. For detection, FITC-conjugated anti-mouse antibody and

[6] ATM, ATR, PI-3K and mTOR. Dr. Graeme Smith, KuDOS Pharmaceuticals, personal communication.

Table 1. Characteristics of CLL cases

Age, y (n = 47), mean (range)	68 (38-91)
Sex (n = 42)	
Male	30
Female	12
Stage at sample collection (n = 48)	
A	22
B	11
C	15
CD38 expression (n = 37)	
>30%	11
<30 %	26
ZAP-70 expression (n = 32)	
>20%	10
<20%	22
Genomic alterations (n = 41)	
del(17p)	7
del(11q)	7
del(17p) and del(11q)	1
Trisomy 12	4
del(17p) and trisomy 12	1
del(13q)	21
Time from diagnosis to treatment, mo (n = 47)	
Mean (95% CI)	49.8 (35-64.6)
No. treated patients	21
No. treatments where known	20
Ex vivo sensitivity chlorambucil (n = 39)	
LC_{50} (μmol/L), mean (range)	10.4 (1-50)
PF_{50}, mean (range)	4 (1-20)
Ex vivo sensitivity fludarabine (n = 44)	
LC_{50} (μmol/L), mean (range)	1 (0.05-8)
PF_{50}, mean (range)	2.2 (1-10)
DNA-PKcs protein level* (n = 31), mean (range)	2.9 (0.17-12.9)

*Protein level was determined by Western blot and expressed as ratio of the actin loading control.

phycoerythrin-conjugated anti-CD19 antibody (Becton Dickinson) were used. A FACScan flow cytometer and CellQuest software (Becton Dickinson) was used to analyze viable $CD19^+$ cells (a positive control of a wild-type p53 case was always included).

DNA damage-inducible γH2AX foci. Following drug or IR treatment, lymphocytes were cytospun onto microscope slides, fixed, and stained as described previously (26). An Olympus BH2-RFCA fluorescence microscope (×40 objective) with Hamamatsu $ORCA_{II}$ BT-1024 cooled CCD camera was used. Separate images were captured for 4,6-diamidine-2-phenyindole and Alexa 594 and composite images were prepared. Image Pro Plus (Media Cybernetics) was used for capture and quantitative analysis to carry out background correction and calculate integrated fluorescence arising from Alexa 594 – stained γH2AX for each nucleus in a field of view [a minimum of 40 nuclei were analyzed (range, 40-100) per treatment].

Comet assay. Following drug or IR treatment, DSB were quantified using the neutral Comet assay (Trevigen) following the manufacturer's protocol. Briefly, cells were washed and resuspended in ice-cold PBS and then mixed with proprietary low melting point agarose (37°C). This mixture was pipetted onto a CometSlide (Trevigen) to gel at 4°C. Following lysis, slides were subjected to electrophoresis at 50 V for 30 min and then fixed, dried, and stained with SYBR Green I. Images were captured on the same system described above (×10 objective) and analyzed using Komet software v 5.5 (Kinetic Imaging).

Western blotting. Whole-cell extracts were prepared and loaded onto Tris-acetate 3% to 8% (v/v) denaturing polyacrylamide gradient gels (Bio-Rad) using standard protocols. Samples were transferred onto Hybond C membrane (Amersham) and probed with antibodies against DNA-PKcs (clone 25-4; Lab Vision), phosphorylated Ser^{2056} DNA-PKcs (Abcam), and actin (loading control, Ab-1; Calbiochem). Anti-mouse (DNA-PKcs and actin) or anti-rabbit (phosphorylated DNA-PKcs) horseradish peroxidase – linked secondary antibodies (Cell Signaling Technology) and ECL reagent (Amersham) were used for detection. A Fuji LAS-3000 luminescent image analyzer system was used for quantification.

Statistical analyses. GraphPad Prism software (http://www.graphpad.com) was used for data analysis. Kaplan-Meier plots were used to examine relationships between TFI (months from diagnosis before receiving first chemotherapy) and several prognostic indicators. The log-rank test was used to calculate P values.

Results

Patient characteristics. Clinical data and prognostic markers (measured at time of sample collection) are summarized in Table 1 (full data for individual patients is in Supplementary Table). Approximately one-third of patients had high levels of CD38 or ZAP-70 and these were mostly distributed among Binet stage B and C cases (none of the stage A cases expressed high levels of CD38). Similarly, del(17p) or del(11q) cases were most commonly stage B or C. Eight of 22 Binet stage A patients had received prior chemotherapy in contrast to 7 of 11 stage B and 11 of 15 stage C [therapy included chlorambucil (n = 17), fludarabine (n = 1), fludarabine/cyclophosphamide (n = 3), and alemtuzumab (n = 2)].

DNA-PKcs autophosphorylation and DNA-PK activity and expression in patient samples. The ability of NU7441 to inhibit DNA-PKcs autophosphorylation (Ser^{2056}) in intact CLL cells was assessed (n = 3). Figure 1A shows representative data for case 33. Preliminary experiments established that, in untreated cells (after 24 h), basal levels of autophosphorylated DNA-PKcs were detectable (presumably due to induction of DNA-PK activity by low levels of spontaneous DNA damage in CLL cells cultured *ex vivo*). Coincubation with 1 μmol/L NU7441 inhibited this autophosphorylation (Fig. 1A). We then examined the effect of chlorambucil and fludarabine treatment. Both agents induced dose-dependent DNA-PK-mediated autophosphorylation of DNA-PKcs that was abrogated by coincubation with NU7441 (Fig. 1A).

Constitutive DNA-PK activity and DNA-PKcs levels were evaluated in untreated CLL samples using the *ex vivo* DNA-PK assay and Western blotting, respectively. There was a strong correlation (Pearson's r = 0.75; P = 0.001) between DNA-PK activity and DNA-PKcs protein levels (Fig. 1B). We therefore used DNA-PKcs levels as a surrogate marker for the comparison of DNA-PK activity between 31 cases. Figure 1C shows a Western blot of DNA-PKcs in samples containing del(17p) or del(11q) and also cases that had del(13q) as the sole abnormality. These data were quantitated by expressing the DNA-PKcs levels as ratios of the actin loading controls, and the results plotted as a bar chart (Fig. 1D). There was a trend toward higher DNA-PKcs levels in the del(17p) and del(11q) cases [mean, 6.4 ± 2.1 for del(17p), 3.2 ± 0.8 for del(11q), and 2.3 ± 0.4 del(13q)]. DNA-PKcs levels were significantly higher in the del(17p) cases compared with cases with del(13q) (P = 0.01).

p53 dysfunction in patient samples. Because of the known association of p53 dysfunction and del(17p) with chemoresistant CLL, flow cytometric analysis was used to stratify cases according to p53 functionality. We assessed 18 cases, including a number that were likely (based on clinical resistance to

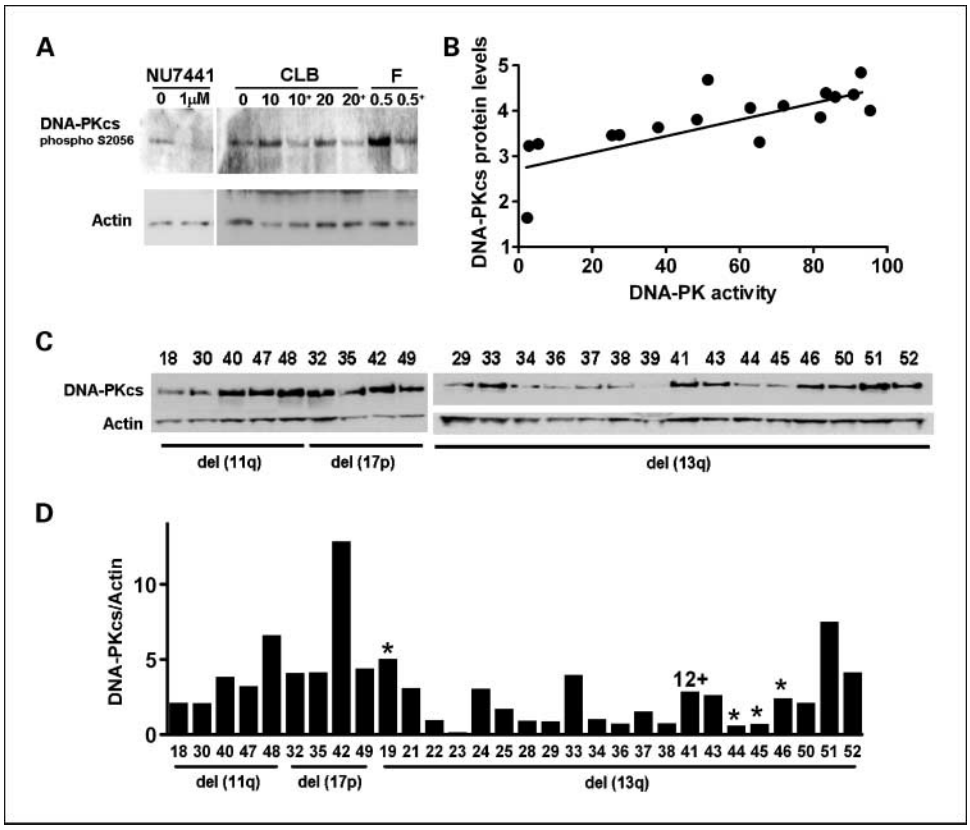

Fig. 1. DNA-PKcs levels are higher in patients with del(11q) and del(17p). *A,* NU7441 inhibits autophosphorylation of DNA-PKcs at Ser^{2056}. Western blot shows results from case 33 after treatment for 24 h in the absence or presence of 1 μmol/L NU7441. Cells were also treated for 24 h with 0, 10, or 20 μmol/L chlorambucil (*CLB*) or 0.5 μmol/L fludarabine (*F*) in the presence (+; after drug concentration) or absence of 1 μmol/L NU7441. *B,* correlation between DNA-PKcs protein levels (expressed as $\log_{10}$, assessed by Western blotting) and enzyme activity assessed using the *ex vivo* DNA-PK assay (expressed as ng DNA-PK as derived from standard curve). *C,* Western blots showing cases with del(17p) or del(11q) and cases with del(13q). *D,* data from Western blots were quantified by expressing DNA-PKcs levels as ratios of the actin loading controls and plotted as a bar chart. *, cases with no chromosomal abnormalities; 12+, trisomy 12. Note: Western blots were repeated with similar results. Sample 39 was considered to be degraded and was not included in the analysis. Due to space limitation, samples 19, 21 to 25, and 28 are not shown in *C*, but their quantification is shown in *D*.

therapy) to harbor defects in the p53 pathway. Prolonged half-life of p53, accompanied by lack of p21 up-regulation following IR, is associated with p53 dysfunction per se (type A), whereas normal basal p53 expression with lack of p21 up-regulation (type B) is associated with ATM dysfunction (25). Patient samples displaying up-regulation of both p53 and p21 following IR treatment are classified as having normal p53 function (type N). From this analysis (data not shown), we identified cases representative of type N (6), type A (6), and type B (6). For 5 of the type A and 3 of the type B cases, cytogenetic analyses were obtained, showing that 4 of 5 cases harbored del(17p) and 2 of 6 harbored del(11q), respectively. We also examined p53 mutations in our patient cohort[7] and noted that type A cases all displayed mutations and thus have dysfunctional p53.

Ex vivo *drug sensitivity*. Dose-response curves established the range of drug sensitivities of cases treated *ex vivo* with chlorambucil or fludarabine. There was considerable variation between cases (Table 1), with the LC_{50} means being 10 and 1 μmol/L for chlorambucil and fludarabine, respectively. There were no significant differences between mean LC_{50} values for the different Binet stages for either drug (data not shown).

LC_{50} values were compared when cases were stratified according to poor prognosis markers. There was no significant difference between the mean LC_{50} values for either drug when low versus high ZAP-70-expressing cases were compared (data not shown). However, cases expressing high levels of CD38 were significantly more resistant to chlorambucil than those expressing low levels (LC_{50} mean, 15.1 ± 4.5 and 5.9 ± 0.8 μmol/L, respectively; $P = 0.01$; Fig. 2A). A similar trend with fludarabine was evident in cases expressing high versus low levels of CD38 (1.4 ± 0.7 and 0.66 ± 0.07 μmol/L, respectively; $P = 0.31$; Fig. 2A). del(17p) cases were significantly more resistant to chlorambucil than the nondeleted cases (14 ± 3.8 and 6.5 ± 0.9 μmol/L, respectively; $P = 0.008$), and there was a trend toward higher LC_{50} values for fludarabine in del(17p) cases versus nondeleted cases (1 ± 0.2 and 0.8 ± 0.08 μmol/L, respectively; $P = 0.25$; Fig. 2B).

Relationships between the LC_{50} values and p53 dysfunction were also investigated. There was a trend toward higher LC_{50} values for chlorambucil and fludarabine in the type B group compared with type N (not significant; Fig. 2C). As would be expected, given the high correspondence between type A and the presence of del(17p), LC_{50} values for the type A cases were significantly higher than the type N cases for chlorambucil (13.5 ± 3.8 and 4.6 ± 2.2 μmol/L, respectively; $P = 0.07$) and fludarabine (1.5 ± 0.2 and 0.8 ± 0.19 μmol/L, respectively; $P = 0.04$). No significant differences were observed for LC_{50} values when cases were grouped as less than or more than the median DNA-PKcs levels (data not shown).

Sensitization by NU7441. Drug combination experiments ($n = 81$) using NU7441 were carried out on 45 cases. Table 1 (and Supplementary Table) show drug sensitivities (LC_{50} values) and the ability of NU7441 to sensitize cells to drugs (PF_{50} values), and Fig. 3 shows representative data from six cases. Figure 3A shows two cases that had normal (type N) p53 function: case 30 [del(11q)] was sensitized by NU7441 to chlorambucil ($PF_{70} = 17$); this case was also sensitized to fludarabine ($PF_{50} = 4$; data not shown), and case 25 [del(13q)]

[7] Crawford et al., to be published independently.

was sensitized to fludarabine. Figure 3B shows two del(11q) cases that were ATM dysfunctional (type B); case 27 was sensitized 4-fold to chlorambucil. For case 48, we compared the abilities of NU7441 and its noninhibitory analogue, NU7742, to enhance the cytotoxicity of fludarabine. Whereas NU7441 sensitized this sample approximately 2-fold, NU7742 had no effect. Figure 3C shows two del(17p) cases that have p53 dysfunction (type A): 1938 was sensitized to chlorambucil and 26 was sensitized to fludarabine by NU7441. For all the cases tested, the range of PF_{50} values observed were 1 to 20 for both fludarabine (n = 44) and chlorambucil (n = 37). Preliminary data (two cases; data not shown) showed that NU7441 also sensitized cells to the alkylating agent, cyclophosphamide.

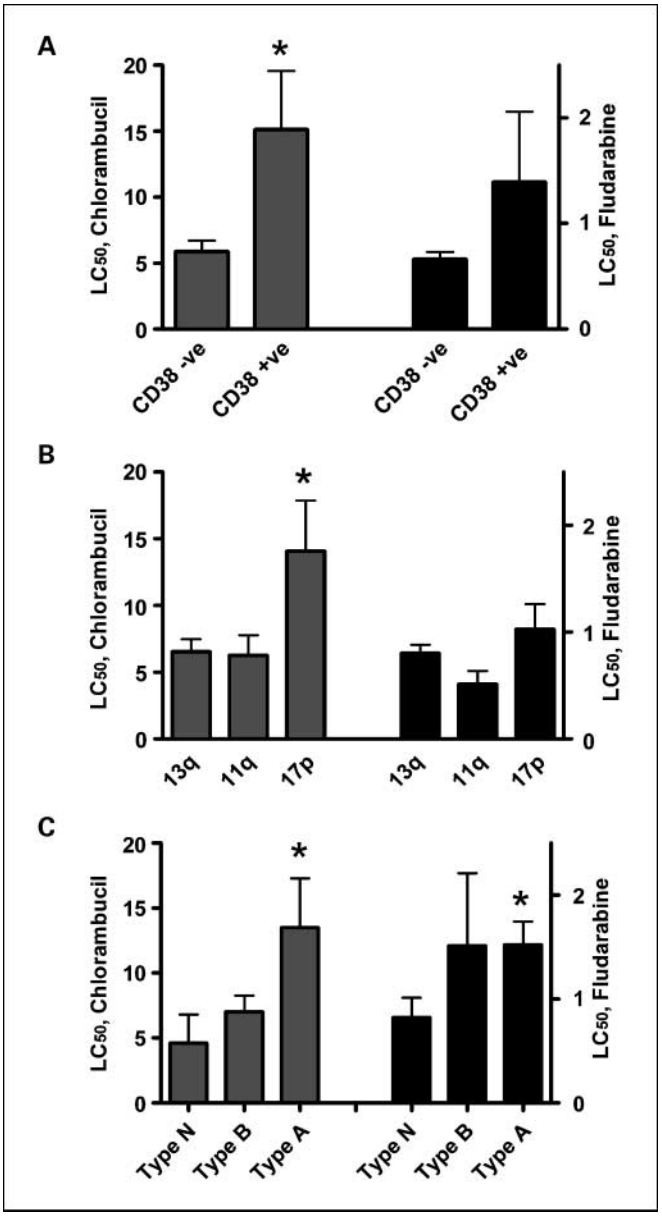

Fig. 2. *Ex vivo* drug sensitivity delineated by prognostic groups. LC_{50} values for chlorambucil (*gray columns, left Y axis*) and fludarabine (*black columns, right Y axis*) grouped according to (*A*) CD38 status (positive if >30% expression); (*B*) deletion status [del(13q) or no deletions versus del(11q) or del(17p)], or (*C*) p53 functionality (type N, normal; type A, associated with p53 mutation; type B, associated with ATM dysfunction). *Columns,* mean; *bars,* SE. *, $P \leq 0.10$.

Caspase-3/7 activation was measured in parallel with viability in CLL cells taken from the same drug-treated cultures. The caspase kit was used as an alternative to Annexin V staining as a measure of apoptosis, because it required fewer cells, and results showed a similar trend to those obtained using Annexin V. Figure 3D shows an increase in caspase-3/7 measured 40 hours after either chlorambucil (case 33) or fludarabine (case 30) treatment. This activation was further increased by coincubation with NU7441, indicating that the decreased viability occurs via increased apoptosis.

Overall, NU7441 increased the sensitivity (PF_{50} > 1) in 24 of 37 (65%) and 20 of 44 (45%) of cases tested with chlorambucil and fludarabine, respectively (NU7441 sensitized cells to both drugs in 13 cases). Clearly, for some cases, NU7441 failed to chemosensitize cells; therefore, we investigated relationships between PF_{50} values and clinical status. Seven of 14 and 8 of 11 Binet stage A cases were sensitized to fludarabine and chlorambucil, respectively. Similarly, 10 of 20 (fludarabine) and 11 of 19 (chlorambucil) Binet stage B/C cases were sensitized. Fifteen of 33 (fludarabine) and 16 of 24 (chlorambucil) del(13q) cases were sensitized. For del(11q) cases, 3 of 5 (fludarabine) and 6 of 8 (chlorambucil) were sensitized. In contrast, for del(17p) cases, 2 of 8 (fludarabine) and 3 of 7 (chlorambucil) were sensitized.

For cases characterized for p53 dysfunction and tested with fludarabine, 4 of 6 type N, 3 of 6 type B, and 1 of 5 type A were sensitized by NU7441. In comparison, 5 of 5 type N, 3 of 5 type B, and 3 of 4 type A were sensitized to chlorambucil. All four del(11q) cases examined (two wild-type ATM function and two with type B ATM dysfunction) were sensitized to one or both drugs by NU7441.

We explored the relationship between the efficacy of NU7441 to potentiate drug-induced cytotoxicity and the presence of high levels of DNA-PKcs. There was no significant difference (e.g., for chlorambucil, P = 0.3) between groups with high compared with low expression of DNA-PKcs in terms of the ability of NU7441 to chemosensitize.

NU7441 increases the persistence of fludarabine-induced DNA damage. Phosphorylation of γH2AX was used as a surrogate marker for DSB to investigate drug-induced DNA damage. We have previously shown high levels of γH2AX foci after treatment with IR (26). As a positive control, CLL cells were treated with 5 Gy IR and this resulted in the rapid formation of γH2AX foci (data not shown). Dose- and time-dependent formation of γH2AX foci was also observed in fludarabine- and chlorambucil-treated cells (6 of 6 and 2 of 3 samples tested, respectively). Figure 4A shows representative images from case 47, after cells had been treated for 40 hours. There were very low levels of γH2AX foci in untreated cells (or cells treated with NU7441 alone), but foci were present in fludarabine-treated cells. NU7441 increased the level of fludarabine-induced foci. Figure 4B shows data for case 53 after levels of γH2AX had been quantified using integrated fluorescence. Fludarabine-induced foci were evident as early as 3 hours and maximal by 24 hours. NU7441 alone had no effect on γH2AX foci, but after 3 hours levels were 3-fold higher in cells that had been treated with fludarabine in the presence of NU7441 compared with fludarabine alone (P < 0.0001), and after 24 hours there was a 1.3-fold increase (P = 0.06). Figure 4C shows that the increase in fludarabine-induced γH2AX foci by NU7441 was mirrored by a corresponding

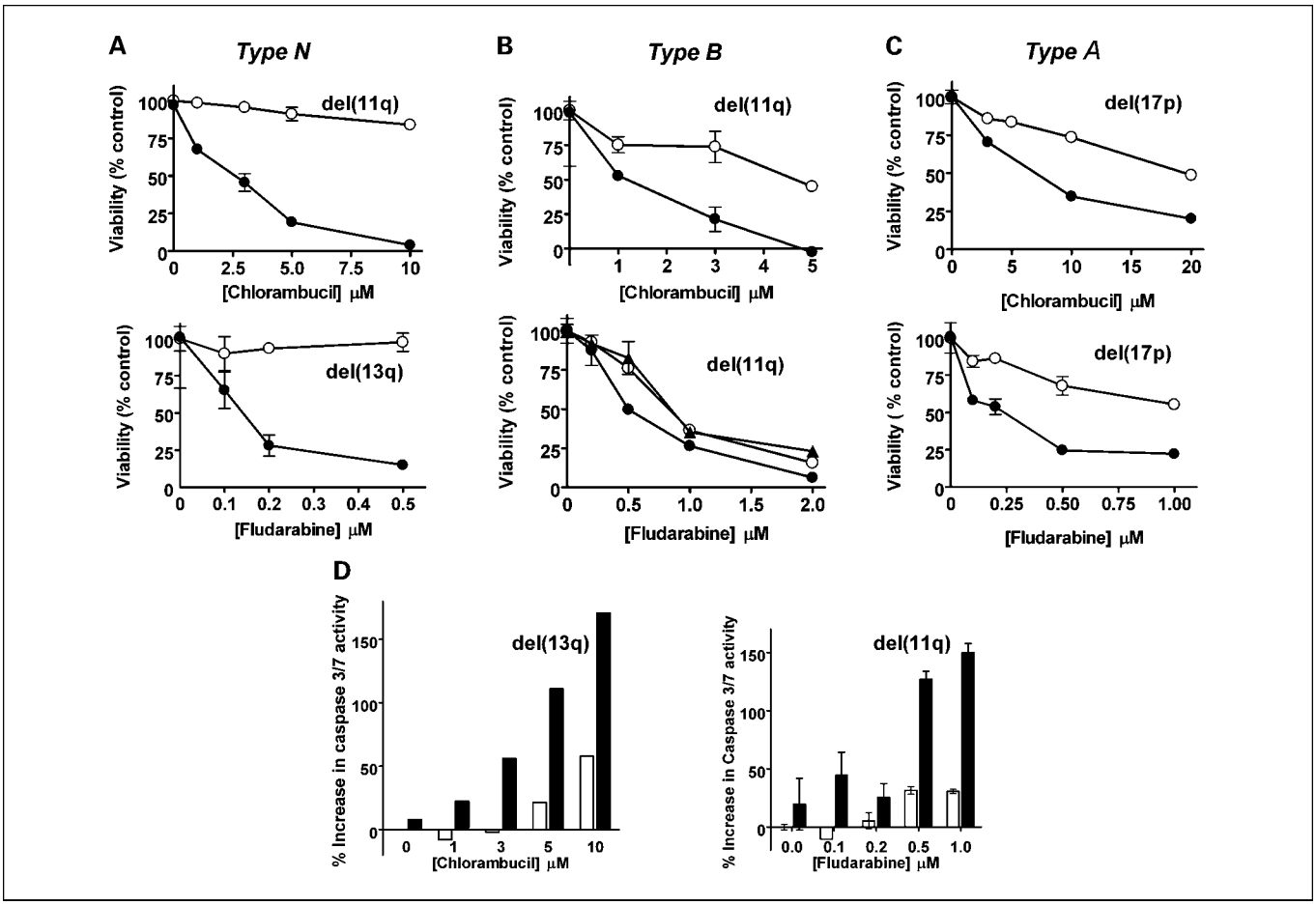

Fig. 3. NU7441 sensitizes cells from poor prognosis CLL patients to fludarabine and chlorambucil. Cells were treated with drug in the presence (●) or absence (○) of NU7441 or (▲) NU7742 and viability was evaluated using the XTT assay (plots for individual cases are shown). *A,* two cases with wild-type p53 function (type N). *B,* two del(11q) cases with ATM dysfunction (type B). *C,* two cases with p53 dysfunction (type A) by virtue of mutation or del(17p). *D,* caspase-3/7 activity was measured after 40-h exposure to drug(s). *White columns,* drug alone; *black columns,* drug + NU7441. Mean ± SE of three to six replicates per CLL case (one replicate for case 33).

decrease in viability (as measured by XTT assay) that was exacerbated by NU7441. Thus, NU7441 increased levels of fludarabine-induced γH2AX foci and correspondingly decreased fludarabine-induced cell death.

Because γH2AX foci may form during other cellular processes, neutral Comet assays were also used to measure DSB formation. As a positive control, we confirmed that IR (5 Gy) induced the formation of DSB (Fig. 4D, case 48). However, when IR-treated cells were incubated in the presence of NU7441, DSB persisted in a time-dependent manner. The level of DSB was higher in NU7441-treated cells 15 minutes post-IR, but after 1 hour most of the DSB were repaired (Fig. 4D). We also investigated the effect of NU7441 on two cases treated with fludarabine. Representative data for case 28 (Fig. 4E) shows that fludarabine induced a dose-dependent increase in DSB that was increased by coincubation with NU7441 (NU7441 per se had no effect on DSB levels). Furthermore, coincubation with the noninhibitory analogue NU7742 had no effect on DSB levels. Taken together, these data are consistent with and substantiate the γH2AX foci results.

Clinical and laboratory correlative data. Kaplan-Meier analysis showed that TFI (defined as time from diagnosis to first chemotherapy) was significantly reduced for del(17p) compared with del(13q) cases (median TFI, 17 and 72 months, respectively; $P = 0.001$; Fig. 5) as well as for del(11q) cases (median TFI, 19 months; $P = 0.01$; Fig. 5). To determine whether DNA-PKcs levels had any bearing on time to treatment, we investigated the effect of high versus low DNA-PKcs levels as defined by protein levels less than or more than median DNA-PKcs levels. Strikingly, TFI was reduced in cases expressing high compared with low DNA-PKcs levels with median TFI of 29 and 75 months, respectively ($P = 0.11$; Fig. 5).

Discussion

The strength of this study has been the ability to relate experimental variables to a cohort of clinically and cytogenetically characterized CLL patient samples. In excellent agreement with the published literature, cases expressing high levels of CD38 (data not shown) or harboring either del(17p) or del(11q) had significantly reduced TFI. No correlation was observed between *ex vivo* resistance (as defined by LC_{50} values) to fludarabine or chlorambucil and Binet stage (data not shown). However, when patient cases were stratified according to CD38 or deletion status, significantly increased resistance to

chlorambucil was observed for the $CD38^+$ and del(17p) cases. There was a trend to higher resistance to fludarabine in del(17p) cases [consistent with Turgut et al. (27)] and to both drugs for the types A and B p53 dysfunctional samples, in line with Sturm et al. (28), who found increased resistance to fludarabine and chlorambucil in cases with p53 mutations.

A limited number of cases were tested for p53 dysfunction as well as for the presence of del(17p) and del(11q). Four of 5 type A cases tested harbored del(17p) and 2 of 3 type B cases harbored del(11q). A discordance in the relationship between del(17p) and p53 dysfunction has been reported (29). Similarly, not all cases carrying ATM mutations harbor del(11q) (ref. 3). Consistent with these reports, our data underscore the fact that gene deletion per se does not identify all cases, which are poor prognosis by virtue of p53 or ATM dysfunction.

Muller et al. (8) showed a correlation between DNA-PK activity and resistance to chlorambucil in CLL patient samples. Further studies attributed an increase in Ku-70/Ku-80 DNA end-binding activity as a mechanism leading to increased DNA-PK activity in resistant CLL cells (11). We observed an excellent correlation between DNA-PK activity and DNA-PKcs protein levels, indicating that increased DNA-PKcs expression makes a major contribution to higher DNA-PK activity. We compared DNA-PKcs levels with specific clinical subtypes and found a wide variation (up to 50-fold) in levels of DNA-PKcs between cases. Strikingly, DNA-PKcs levels were significantly higher in del(17p) cases [compared with del(13q)] and markedly higher in del(11q) cases. Consistent with this, DNA-PKcs overexpression was observed in mutant, compared with wild-type p53 CLL, as shown by microarray analysis (30). Furthermore, Sah et al. (31) reported that induction of wild-type p53 into a p53-null cell line suppressed DNA-PKcs expression. Although we have not fully characterized the p53 mutational status by sequencing in our del(17p) cases, the majority were type A and are therefore predicted to have p53 mutations in the remaining allele. We were unable to conclude that the chemoresistance that we observed was mediated by increased DNA-PKcs levels per se, because a disproportionate number of the samples with high levels harbored del(17p) or del(11q).

The ability of NU7441 to sensitize CLL cells to drugs was assessed comprehensively. Overall, NU7441 sensitized 65% of cases to chlorambucil and 45% to fludarabine, with considerable variations in the PF_{50} values. These percentages did not alter significantly when cases were grouped according to Binet stage, indicating the potential of targeting DNA-PK at all stages of disease. We examined the relationship between efficacy of NU7441 to potentiate drug-induced cytotoxicity and the levels of DNA-PKcs. The proportion of cases that were chemosensitized by NU7441 was similar in the groups with high compared with low expression of DNA-PKcs. However, when cases were stratified according to deletion status, all of del(11q) or del(17p) cases had high DNA-PKcs, 3 of 6 of the del(17p) cases were sensitized to chlorambucil, and only 1 of 7 was sensitized to fludarabine. It has been shown previously that fludarabine-induced cytotoxicity is p53 dependent (5); hence, the lack of sensitization by NU7441 in this context is not

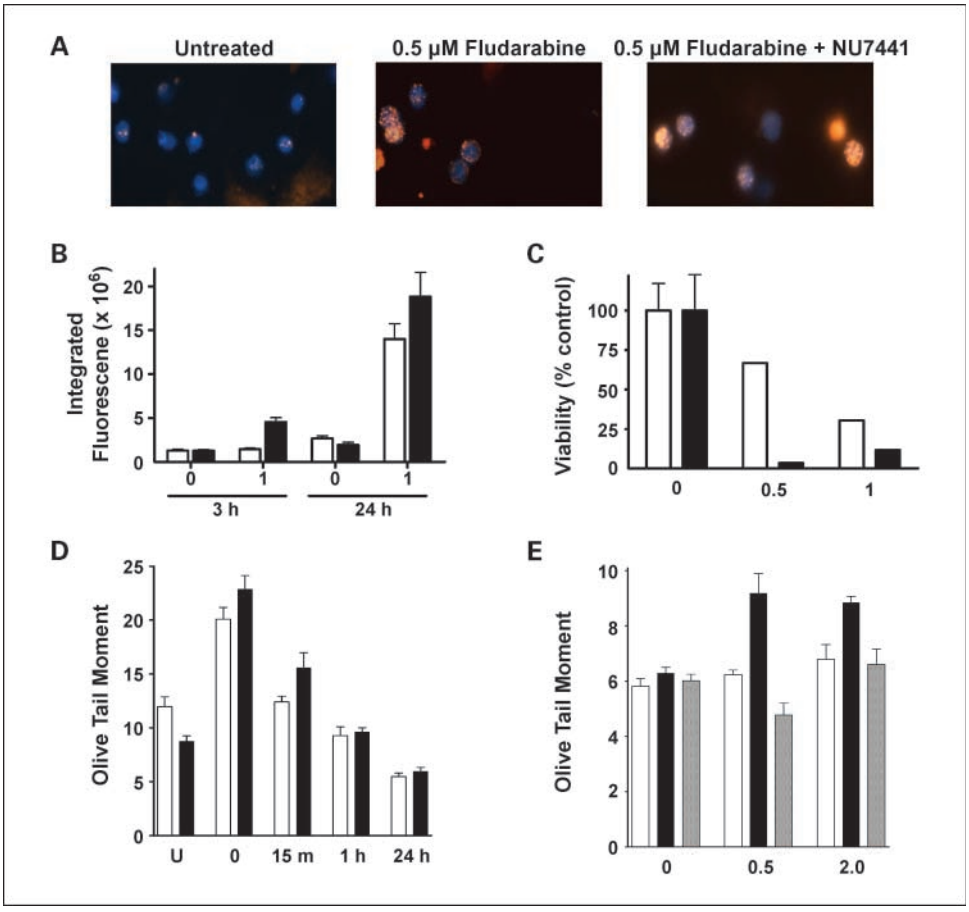

Fig. 4. NU7441 increases fludarabine-induced DSB in CLL cells. CLL cells from case 47 were treated with fludarabine (40 h) in the presence or absence of NU7741 before cytospin and staining for γH2AX foci. *A,* representative images (×20) show untreated cells (images were similar after treatment with NU7441 alone) or cells after treatment with fludarabine in the presence and absence of NU441. *B,* for case 53, quantification (integrated fluorescence) after 3- or 24-h treatment with fludarabine in the absence (*white columns*) or presence (*black columns*) of NU7441. *C,* corresponding decrease in viability (case 53) 5 d following treatment with fludarabine in the absence (*white columns*) or presence (*black columns*) of NU7441. *D,* cells from case 48 were treated with 5 Gy IR and allowed to repair (15 min, 1 h, or 24 h) in the absence (*white columns*) or presence (*black columns*) of NU7441. *E,* case 28 after treatment for 24 h with 0.5 or 2 μmol/L fludarabine in the absence (*white columns*) or presence of NU7441 (*black columns*) or NU7742 (*gray columns*). Olive tail moment was calculated. Mean ± SE.

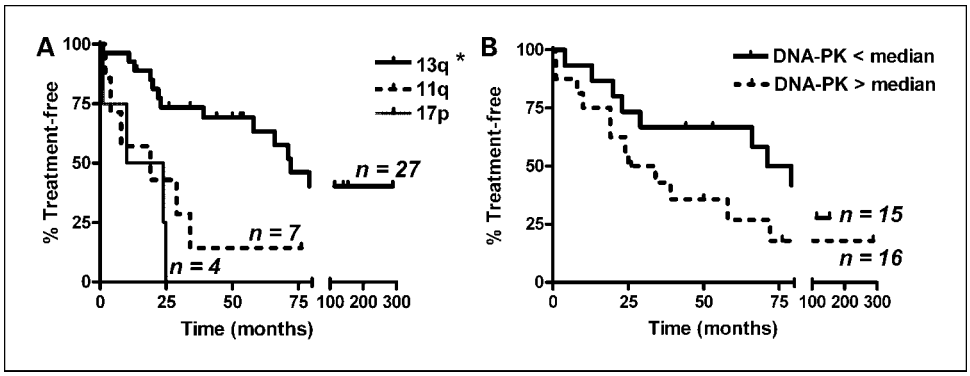

Fig. 5. *A,* DNA-PKcs expression predicts short TFI. TFI (from time of diagnosis) in relation to deletion status [del(13q) or no abnormalities; *solid line*] versus 11q (*dotted line*) or 17p (*gray line*) deletions. *B,* DNA-PKcs expression [protein levels less than median (*solid line*) versus more than median (*dotted line*)]. The log-rank test was used to determine statistical significance.

surprising. By contrast, not only were the majority of del(11q) cases sensitized to drugs by NU7441, but in these cases we saw high levels of potentiation (up to 4-fold for fludarabine and 20-fold for chlorambucil). This raises the question of whether dysfunction of one DSB repair pathway (a defect in homologous recombination repair resulting from ATM dysfunction) may be associated with up-regulation of a complementary pathway (increased nonhomologous end joining mediated by increased DNA-PK activity).

A previous study (19) showed that the DNA-PK inhibitor NU7026 increased chlorambucil-induced DSB in CLL and that this correlated with inhibition of DNA-PK and sensitization to chlorambucil. Consequently, our study concentrated on the effect of the more potent and specific NU7441 on DSB levels using the less documented fludarabine. Both γH2AX foci data and Comet analyses concurred: fludarabine treatment resulted in a dose-dependent increase in DSB levels that were increased by coincubation with NU7441. Overall, these data support the contention that fludarabine induces DSB formation in CLL lymphocytes and the repair of these breaks is mediated by DNA-PK.

When cases were grouped according to high versus low DNA-PKcs levels, there was an evident trend to reduced TFI in the high DNA-PKcs group. A plausible hypothesis is that increased activity of repair mediated by nonhomologous end joining (an error-prone DSB repair pathway, resulting in the accumulation of deletions at repair sites) is likely to confer a mutator phenotype, resulting in chromosomal instability, and hence promoting disease progression. There is a need for effective therapies in high risk CLL, and our study shows that a DNA-PK inhibitor sensitizes cells from poor prognosis CLL patients to currently used drugs. Thus, targeted inhibition of DNA-PK may prove a valuable addition to current therapeutic regimes.

Disclosure of Potential Conflicts of Interest

No potential conflicts of interest were disclosed.

Acknowledgments

We thank all the patients who kindly donated samples and Drs. Caroline Richardson and Graeme Smith (KuDOS Pharmaceuticals) for advice and discussion.

References

1. Döhner H, Stilgenbauer S, Benner A, et al. Genomic aberrations and survival in chronic lymphocytic leukaemia. N Engl J Med 2000;343:1910–6.
2. Kay NE, O'Brien SM, Pettitt AR, Stilgenbauer S. The role of prognostic factors in assessing "high-risk" subgroups of patients with chronic lymphocytic leukemia. Leukemia 2007;21:1885–91.
3. Austen B, Powell JE, Alvi A, et al. Mutations in the ATM gene lead to impaired overall and treatment-free survival that is independent of IGVH mutation status in patients with B-CLL. Blood 2005;106:3175–82.
4. Johnston JB, Daeninck P, Verburg L, et al. p53, MDM-2, BAX and BCL-2 and drug resistance in chronic lymphocytic leukemia. Leuk Lymphoma 1997; 26:435–49.
5. Ashtusosh Rao V, Plunkett W. Activation of a p53-mediated apoptotic pathway in quiescent lymphocytes after inhibition of DNA repair by fludarabine. Clin Cancer Res 2003;9:3204–12.
6. Christodoulopoulos G, Malapetsa A, Schipper H, Golub E, Radding C, Panasci LC. Chlorambucil induction of HsRad51 in B-cell chronic lymphocytic leukemia. Clin Cancer Res 1999;5:2178–84.
7. Andersson BS, Sadeghi T, Siciliano MJ, Legerski R, Murray D. Nucleotide excision repair genes as determinants of cellular sensitivity to cyclophosphamide analogs. Cancer Chem Pharmacol 1996;38:406–16.
8. Muller C, Chistodoulopoulos G, Salles B, Panasci L. DNA-dependent protein kinase activity correlates with clinical and *in vitro* sensitivity of chronic lymphocytic leukemia lymphocytes to nitrogen mustards. Blood 1998;92:2213–9.
9. Muller C, Calsou P, Salles B. The activity of the DNA-dependent protein kinase (DNA-PK) complex is determinant in the cellular response to nitrogen mustards. Biochimie 2000;82:25–8.
10. Collis SJ, DeWeeseTL, Jeggo PA, Parker AR. The life and death of DNA-PK. Oncogene 2005;24:949–61.
11. Deriano L, Guipaud O, Merle-Beral H, et al. Human chronic lymphocytic leukemia B cells can escape DNA damage-induced apoptosis through the nonhomologous end-joining DNA repair pathway. Blood 2005; 105:4776–83.
12. Yamauchi T. Nowak BJ. Keating MJ. Plunkett W. DNA repair initiated in chronic lymphocytic leukemia lymphocytes by 4-hydroperoxycyclophosphamide is inhibited by fludarabine and clofarabine. Clin Cancer Res 2001;7:3580–9.
13. Izzard RA, Jackson, SP, Smith, GC. Competitive and non-competitive inhibition of the DNA-dependent protein kinase. Cancer Res 1999;59:2581–6.
14. Rosenzweig KE, Youmell MB, Palayoor ST, Price BD. Radiosensitization of human tumor cells by the phosphatidylinositol 3-kinase inhibitors wortmannin and LY294002 correlates with inhibition of DNA-dependent protein kinase and prolonged G_2-M delay. Clin Cancer Res 1997;3:1149–56.
15. Boulton S, Kyle S, Durkacz BW. Mechanisms of enhancement of cytotoxicity in etoposide and ionising radiation-treated cells by the protein kinase inhibitor wortmannin. Eur J Cancer 2000;36:535–41.
16. Vlahos CJ, Matter WF, Hui KY, Brown RF. A specific inhibitor of phosphatidylinositol 3-kinase, 2-(4-morpholinyl)-8-phenyl-4H-1-benzopyran-4-one (LY294002). J Biol Chem 1994;269:5241–8.
17. Veuger SJ, Curtin NJ, Smith GC, Durkacz BW. Effects of novel inhibitors of poly(ADP-ribose) polymerase-1 and the DNA-dependent protein kinase on enzyme activities and DNA repair. Oncogene 2004; 23:7322–9.
18. Willmore E, de Caux S, Sunter NJ, et al. A novel DNA-dependent protein kinase inhibitor, NU7026, potentiates the cytotoxicity of topoisomerase II poisons used in the treatment of leukemia. Blood 2004; 103:4659–65.
19. Amrein L, Loignon M, Goulet A-C, et al. Chlorambucil cytotoxicity in malignant B lymphocytes is synergistically increased by 2-(morpholin-4-yl)-benzo[*h*]chomen-4-one (NU7026)-mediated inhibition of DNA double-strand break repair via inhibition of DNA-dependent protein kinase. J Pharmacol Exp Ther 2007;321:848–55.
20. Hardcastle IR, Cockcroft X, Curtin NJ, et al. Discovery of potent chromen-4-one inhibitors of the DNA-dependent protein kinase (DNA-PK) using a small-molecule library approach. J Med Chem 2005;48: 7829–46.

21. Zhao Y, Thomas HD, Batey MA, et al. Preclinical evaluation of a potent novel DNA-dependent protein kinase inhibitor NU7441. Cancer Res 2006;66:5354–62.

22. Dignum HM, Summerfield GP, Proctor SJ, Mainou-Fowler T. Quantification of CD38 expression in B-cell chronic lymphocytic leukemia (B-CLL): a comparison between antibody binding capacity (ABC) and relative median fluorescence (RMF). Br J Haematol 2002;118:755–61.

23. Gibbs G, Bromidge T, Howe D, Hopkins J, Johnson S. Comparison of flow cytometric methods for the measurement of ZAP-70 expression in a routine diagnostic laboratory. Clin Lab Haem 2005;27:258–66.

24. Griffin RJ, Fontana G, Golding BT, et al. Selective benzopyranone and pyrimido[2,1-*a*]isoquinolin-4-one inhibitors of DNA-dependent protein kinase: synthesis, structure-activity studies, and radiosensitization of a human tumor cell line *in vitro*. J Med Chem 2005;48:569–85.

25. Carter A, Lin K, Sherrington PD, Pettitt AR. Detection of p53 dysfunction by flow cytometry in chronic lymphocytic leukaemia. Br J Haem 2004;127:425–8.

26. Cowell IG, Durkacz BW, Tilby MJ. Sensitization of breast carcinoma cells to ionizing radiation by small molecule inhibitors of DNA-dependent protein kinase and ataxia telangiectasia mutated. Biochem Pharmacol 2005;71:19–20.

27. Turgut B, Vural O, Pala FS, et al. 17p deletion is associated with resistance of B-cell chronic lymphocytic leukemia cells to *in vitro* fludarabine-induced apoptosis. Leuk Lymphoma 2007;48:311–20.

28. Sturm I, Bosanquet AG, Hermann S, Güner D, Dörken B, Daniel PT. Mutation of p53 and consecutive selective drug resistance in B-CLL occurs as a consequence of prior DNA-damaging chemotherapy. Cell Death Differ 2003;10:477–84.

29. Carter A, Lin K, Sherrington PD, et al. Imperfect correlation between p53 dysfunction and deletion of TP53 and ATM in chronic lymphocytic leukemia. Leukemia 2006;20:737–40.

30. Stankovic T, Hubank M, Cronin D, et al. Microarray analysis reveals that *TP53*- and *ATM*-mutant B-CLLs share a defect in activating proapoptotic responses after DNA damage but are distinguished by major differences in activating prosurvival responses. Blood 2004;103:291–300.

31. Sah NK, Munshi A, Nishikawa T, Mukhopadhyay T, Roth JA, Meyn RE. Adenovirus-mediated wild-type p53 radiosensitizes human tumor cells by suppressing DNA repair capacity. Mol Cancer Ther 2003;2:1223–31.